Supplementary information for:

Differential pH as a method for increasing cell potential in organic aqueous flow batteries

Amirreza Khataee[a], Kristina Wedege[a], Emil Dražević[a], and Anders Bentien*[a]

[a]Hangøvej 2, 8200 Aarhus (Denmark), Department of Engineering, Aarhus University.

*Corresponding author. E-mail: bentien@eng.au.dk

Table of Contents

S1: Redox flow battery setup

The RF cell charging/discharging experiments were conducted in a single flow (Fig. S1a). The RF cell is a homemade cell and consists of carbon paper electrodes, end plates, current collectors and a cation exchange membrane. In order to facilitate current collection, solid gold plated copper plates were employed. Graphite plates with interdigitated flow field were used as bipolar plates. Carbon papers were used as electrodes on both sides of the cell. Nafion-117 was adopted as a cation exchange membrane and Viton and Teflon gaskets were used for sealing the cell assembly. To assemble the cell, current collectors were screwed together by eight bolts with bipolar plates, electrodes and gaskets in between. For circulating the electrolytes through the cell, two Grundfos DDA pumps with Teflon tubing were utilized. The solutions were purged with nitrogen before use. Charge/discharge studies were carried out under constant current densities with upper limit of 1.6 V during charge and lower limit of 0.2 V during discharge, respectively. A battery testing system (BTS-5V3A) was used for charging and discharging the cell and data collecting.

Fig. S1 a) Cell used for battery tests; b) Photo of the experimental setup of the Na_2AQDS/Bromide redox flow.

S2: Conductivity measurements

Concentration of NH_4Br (M)	Conductivity (mS cm^{-1})
0.5	55
1	108
2	206
3	295
4	367
5	433
6	499

Concentration of H_2SO_4 (M)	Conductivity (mS cm^{-1})
0.5	278
1	506
2	686
3	787
4	802
5	780
6	581

S3: Aqueous disproportionation reactions of bromine

Bromine disproportionates in water giving the species Br_2, Br^-, Br_3^-, HBrO, BrO^-, $HBrO_3$, and BrO_3^-. The most important equilibria are[1]:

Disproportionation to hypobromous acid (pKa = 8.69 [2]):

$$Br_2 + H_2O \rightleftharpoons HBrO + H^+ + Br^-$$

$$K_{eq} = 7.2 \cdot 10^{-9}\ [3]$$

Hypobromous acid further disproportionate to bromate (bromic acid pkA = -2 [2]):

$$3BrO^- \rightleftharpoons 2Br^- + BrO_3^-$$

$$K_{eq} = 10^{15}\ [3]$$

Tribromide arises when bromide and bromide is present, and this equilibrium is responsible for the large solubility of bromine:

$$Br^- + Br_2 \rightleftharpoons Br_3^-$$

$$K_{eq} = 16\ [4]$$

In a 0.3 M bromine-water solution, if all equilibria are taken into account, the pH of the solution should be 2.66[5] which fits well with the measured **2.69.** From these the sum of inactivated bromine (in terms of the battery conditions) compounds can be calculated[5].

$$pH = -\log([HBrO] + 2[BrO^-] + 5[HBrO_3] + 6[BrO_3^-]) = -\log(\sum[\text{Disproportionation products}])$$

$$\rightarrow \sum[\text{Disproportionation products}] = 0.002\ \text{M}$$

The addition of 2 M NH_4Br to the 0.3 M bromine-water solution a) causes the concentration of tribromide to increase, b) drives the equilibria away from bromate and hypobromous acid and as a consequence, the pH increases to **2.83**. Before the battery test in Figure 6 of the main paper, the pH of the catholyte was decreased to 1.5 with HBr as a starting condition, and during 100 cycles the pH increases to 2.1. Calculating the sum of the concentration of disproportionation products from this gives:

$$\sum[\text{Disproportionation products}] = 0.008\ \text{M}$$

So, there is a constant amount of disproportionation products in the catholyte, but it is too small (1.6% of 0.5 M Br_2) to solely explain the capacity loss in the battery which was 10% over 200 cycles.

S4: RDE studies of Na_2AQDS at pH 0, 7 and 8

In order to compare diffusion coefficient and kinetics constant of Na_2AQDS at pH 0, 7 and 8, linear sweep voltammetry (LSV) study of 1 mM Na_2AQDS in 1 M H_2SO_4, 2 M NH4Br and 2 M NH4Br&0.05 M sodium carbonate was carried out at room temperature using a rotating disk electrode system as described in the main paper. LSV measurements were performed at constant potential sweep rate of 10 mV s^{-1} using a freshly polished 5 mm diameter glassy carbon disk electrode as a working (rotating) electrode, a platinum-wire counter electrode and Ag/AgCl reference electrode. The voltage was linearly swept while the rotating electrode was rotated at 200, 300, 400, 500, 700, 900, 1200, 1600, 2000 and 2500 r.p.m.

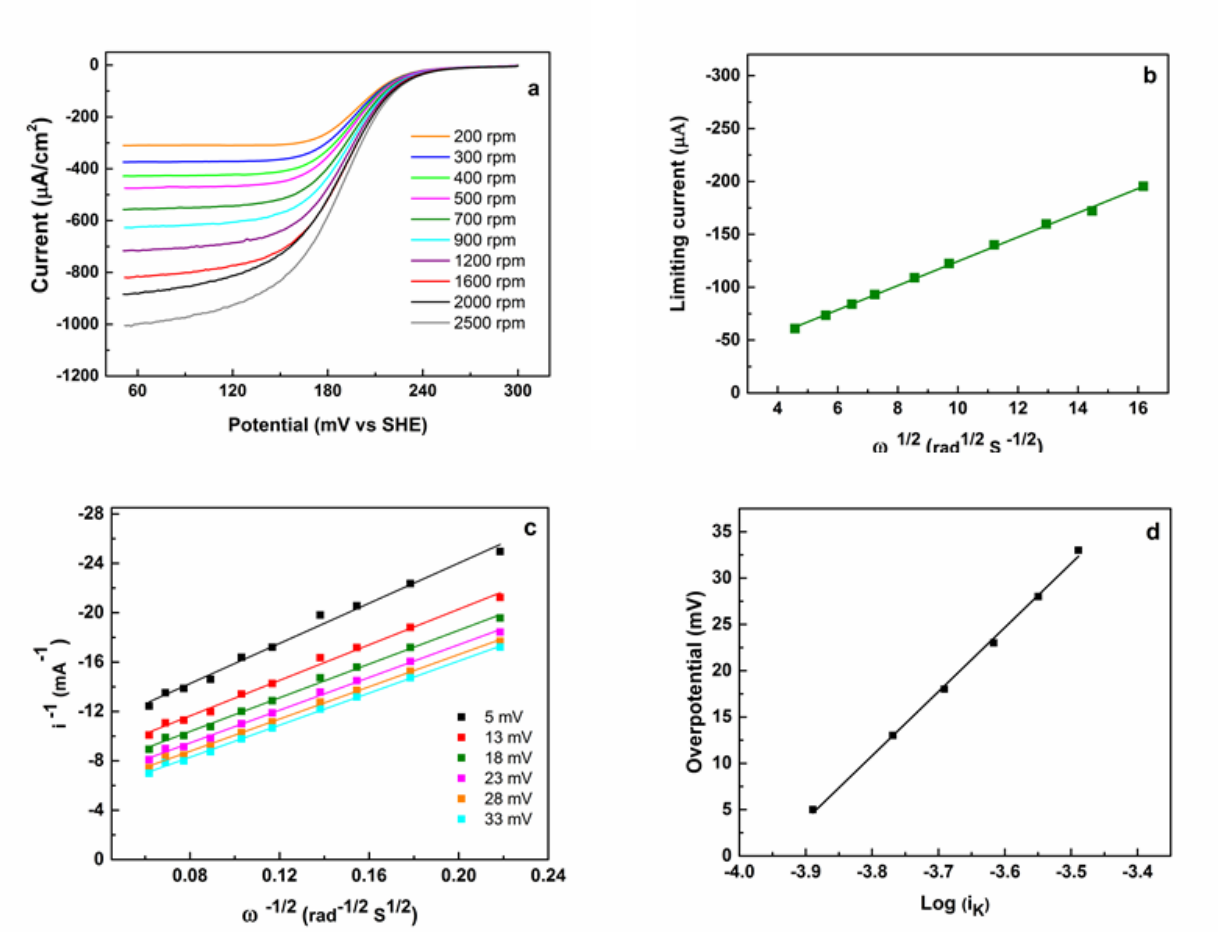

Fig. S4.I (a) Linear sweep voltammograms of 1 mM Na_2AQDS in 1 M H_2SO_4 at scan rate of 10 mVs^{-1} at pH=0 collected with the rotating glassy carbon disk electrode; (b) Levich plot using RDE – Variation of limiting current with square root of rotation rates for Na_2AQDS, the fitted line has a slope of 11 μA $s^{1/2}$ $rad^{-1/2}$, giving D= 3.48×10^{-6} cm^2 s^{-1}; (c) Koutecky´–Levich plot using RDE and derived from six different Na_2AQDS potentials; (d) Fit of Butler–Volmer equation. i_K is the current extrapolated from the zero-intercept of Fig. S4.I(c). Best-fit line has the equation y = 69.25 (x + 3.95). This yields α = 0.431 and k^0= 5.8 × 10^{-3} cm s^{-1}.

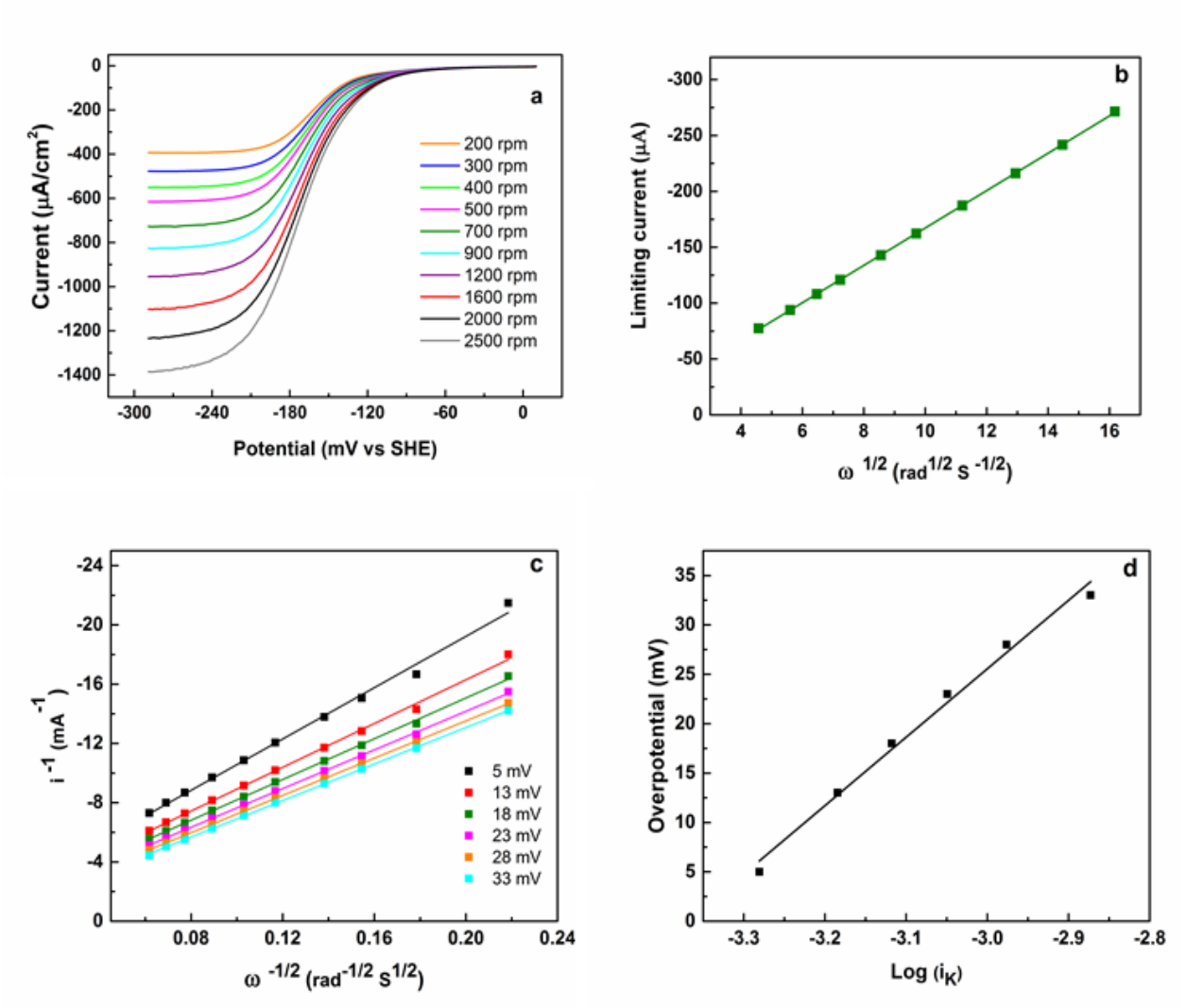

Fig. S4.II (a) Linear sweep voltammograms of 1 mM Na_2AQDS S in 2 M NH_4Br at scan rate of 10 mVs^{-1} at pH=7 collected with the rotating glassy carbon disk electrode; (b) Levich plot using RDE – Variation of limiting current with square root of rotation rates for Na_2AQDS, the fitted line has a slope of 16 μA $s^{1/2}$ $rad^{-1/2}$, giving D= 6.49×10^{-6} cm^2 s^{-1}; (c) Koutecky´–Levich plot using RDE and derived from six different Na_2AQDS potentials; (d) Fit of Butler–Volmer equation. i_K is the current extrapolated from the zero-intercept of Fig. S4.II(c). Best-fit line has the equation y = 69.29 (x + 3.36). This yields α = 0.426 and k^0= 2.1 × 10^{-2} cm s^{-1}.

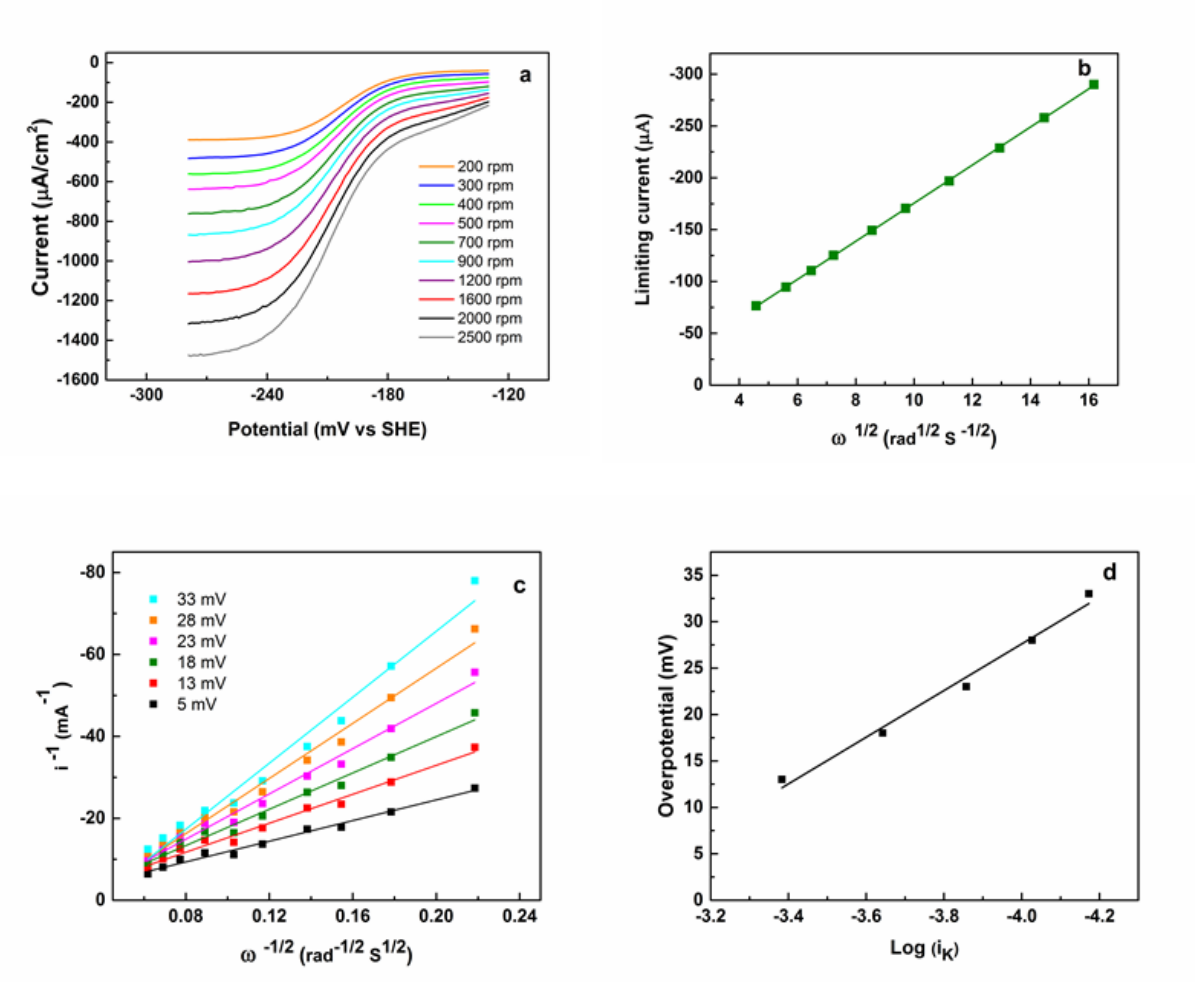

Fig. S4.III (a) Linear sweep voltammograms of 1 mM Na_2AQDS S in 2 M NH_4Br and 0.05 M Na_2CO_3 at scan rate of 10 mVs^{-1} at pH=8 collected with the rotating glassy carbon disk electrode; (b) Levich plot using RDE – Variation of limiting current with square root of rotation rates for Na_2AQDS, the fitted line has a slope of 18.4 $\mu A\ s^{1/2}\ rad^{-1/2}$, giving D= 7.5×10^{-6} $cm^2\ s^{-1}$; (c) Koutecky´–Levich plot using RDE and derived from six different Na_2AQDS potentials; (d) Fit of Butler–Volmer equation. i_K is the current extrapolated from the zero-intercept of Fig. S4.III(c). Best-fit line has the equation y = 28.5 (x + 3.2). This yields $\alpha = 0.405$ and $k^0 = 7.1 \times 10^{-2}$ cm s^{-1}.

The number of electrons transferred during AQDS reduction was measured versus 1-eletron transfer reference solution of 1 mM $Fe(CN)_6^{3-}$ as can be seen in Fig. S4.IV. The background capacitive current was evaluated by 3rd degree polynomial fitting as indicated with red dotted lined and subtracted the current before integration to give the apparent capacity in mC (blue numbers). More precisely, Fig. S4.VI shows that 1.44 electrons (72% of theoretical value which is 2 electrons) are transferred per AQDS. The diffusion coefficients are similar (6.49×10-6 $cm^2\ s^{-1}$ for AQDS and 7.6×10^{-6} for $Fe(CN)_6^{3-}$ so the integrated areas provide a reasonable comparison of the electron/charge relationship. In order to confirm that the current densities at pH = 7 and 8 are higher than pH = 0, a comparison of LSVs at 3 different rotation rates is indicated in Fig. S4.V.

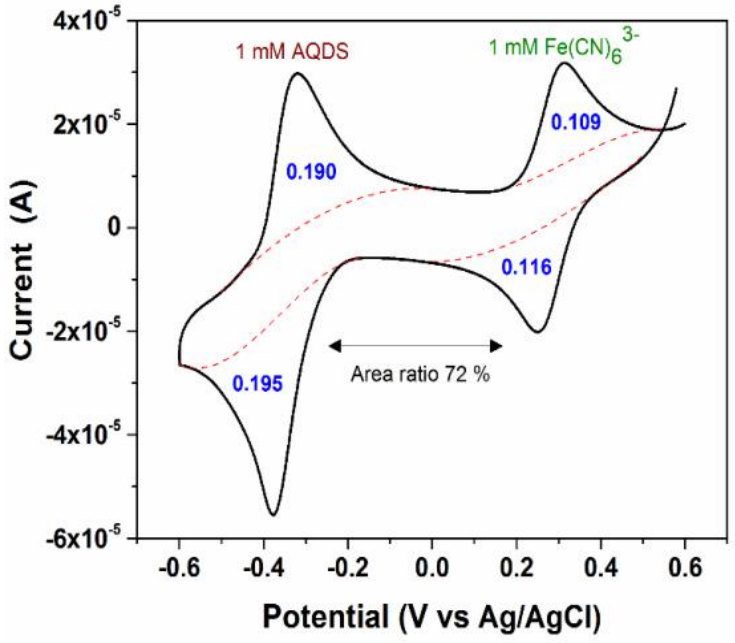

Fig. S4.IV Cyclic voltammograms at 25 mVs^{-1} on a glassy carbon electrode of 1 mM of Na_2AQDS in 2 M NH_4Br (left CV) and 1 mM $Fe(CN)_6^{3-}$ (right CV). The red dotted lines determine the background currents subtracted the curents before integration to give the apparent capacity (blue numbers) of reach oxidation or reduction process.

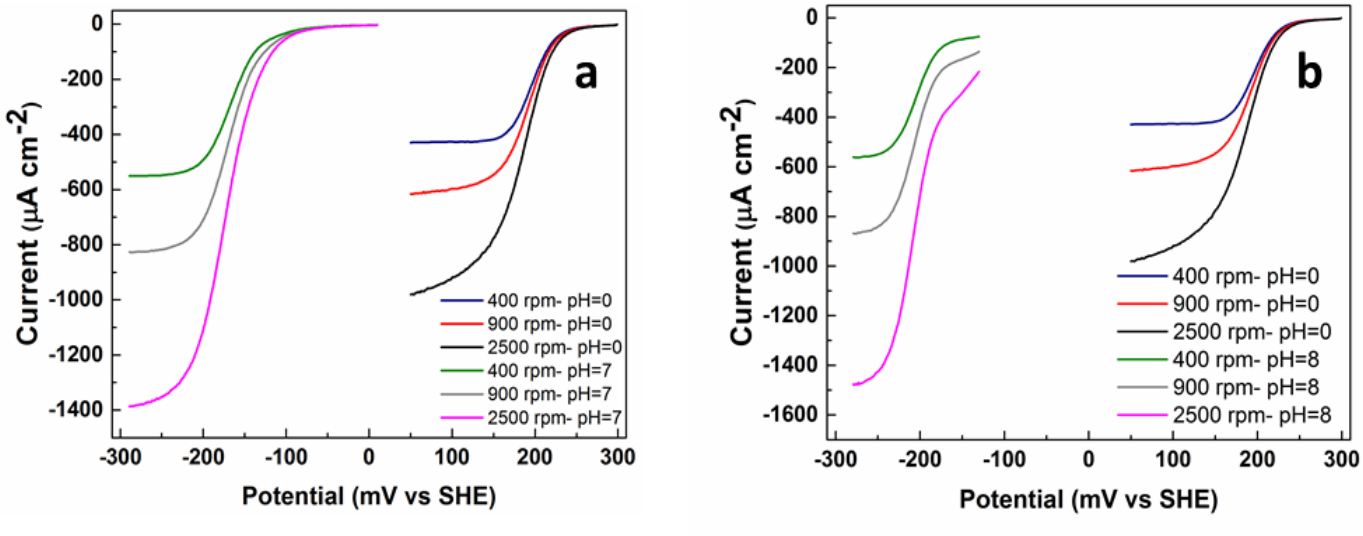

Fig. S4.V a) Linear sweep voltammograms of 1 mM Na_2AQDS in 1 M H_2SO_4, 2 M NH_4Br and 2 M NH_4Br/0.05 M Na_2CO_3 at scan rate of 10 mVs^{-1} and rotation rates of 400, 900 and 2500 rpm at pH = 0, 7 and 8, respectively. Collected with the rotating glassy carbon disk electrode.

RDE tests indicate that high at high pH values, Na_2AQDS has higher standard heterogeneous electron transfer rate constant (k^0). Another test was conducted to prove the results of RDE experiments. Therefore, to corroborate the enhanced reduction properties of Na_2AQDS at pH 8 than in acidic, a CV peak separation analysis were made using 30 mM solutions in 1 M H_2SO_4 or 2 M NH_4Br. The CVs were recorded at scan rates from 50-1000 mV/s on a 3 mm glassy carbon electrode polished identically with 0.05 µm alumina on a micro cloth. The peak separation ΔE_{pp} at high scan rates in the electrochemically (kinetically) irreversible limit is above 59 mv and given by[6]:

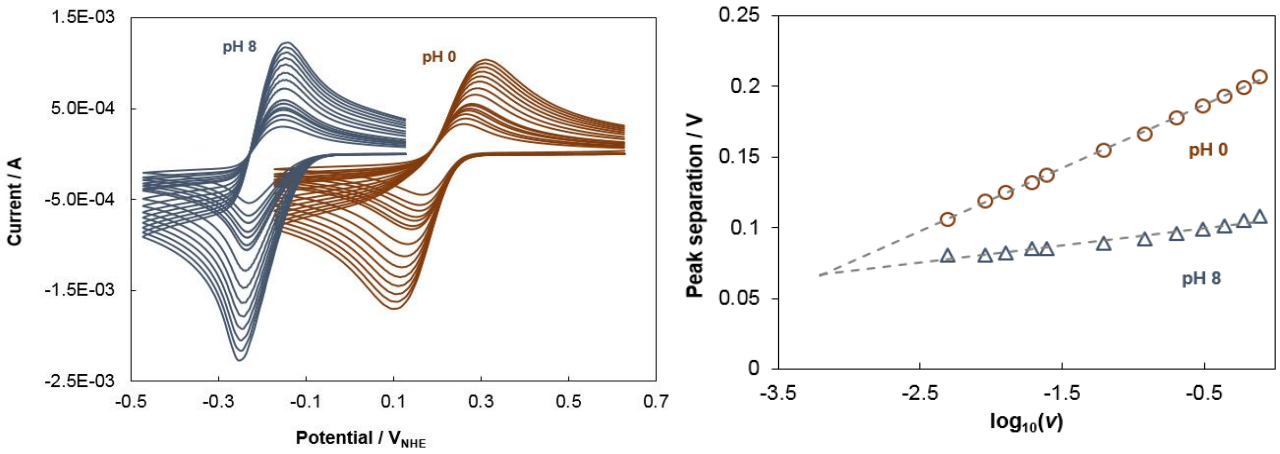

Fig. S4.VI Series of CVs of 30 mM Na_2AQDS recorded at pH 0 and pH 8, respectively (left) and the observed peak-to-peak separation as a function of the logarithm of the scan rate (right).

$$\Delta E_{pp} = \frac{59.4}{\alpha} \cdot \log_{10}(v) + \text{constant} \quad \text{at } 298\ K$$

As seen in Figure above the peak separation increases much more with scan rate at pH 0 than at pH 8, but the peak currents at pH 8 are higher than at pH 0, indicating more favorable kinetics of the reduction at the glassy carbon electrode.

S5: pH titration NMR spectra of Na_2AQDS

As supporting information for the conclusions about the buffer capacity and composition of the redox solutions, a range of different pH titrations have been made and presented in the following. With respect to CO_2 bound in Na_2AQDS the same conclusions as the ones in ref. [32] (T. J. Carney, S. J. Collins, J. S. Moore and F. R. Brushett, Chemistry of Materials, 2017.) in the main text were reached. Proton exchanged Na_2AQDS was prepared by flushing twice through an Amberlyst 15 H+ ion-exchange column. A Metrohm 916 Ti-Touch autotitrator was used for titration.

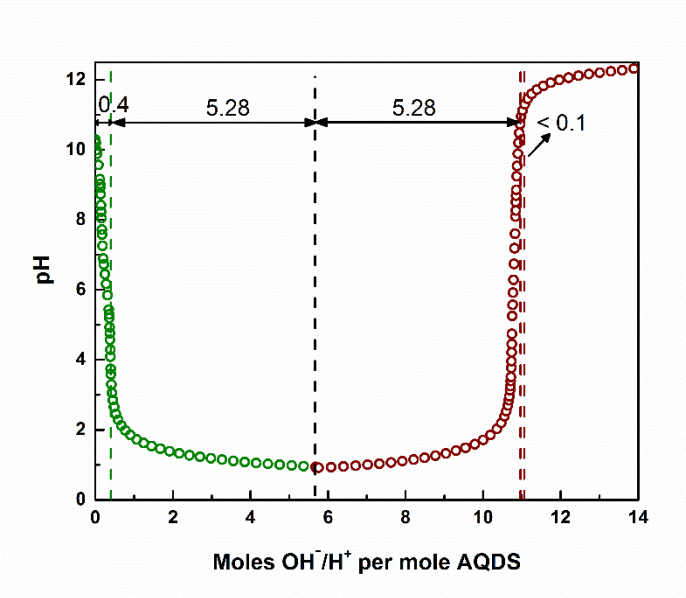

Fig. S5.I Titration curve of oxidised 0.05M Na_2AQDS (combi-blocks) with 0.5 M HCl (green solid line) and reverse titration of same solution with 0.5 M NaOH (red solid line).

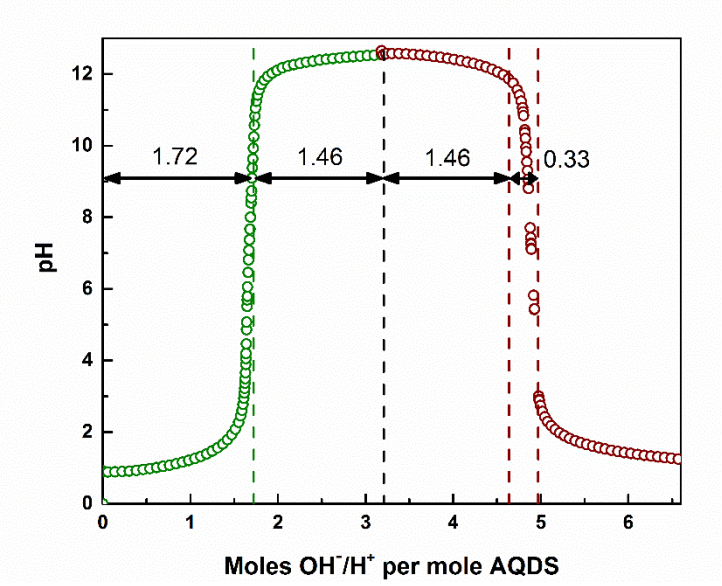

Fig. S5.II Titration curve of oxidised 0.2M H_2AQDS with 0.5 M NaOH (green solid line) and reverse titration of the same solution with 0.5 M HC (red solid line).

In order to investigate the properties of Na_2AQDS further, material from two different suppliers were tested Combi-Blocks (95% pure) and TCI (97% pure). A comparison of the two Na_2AQDS compounds from Combi-Blocks (95% pure) and TCI (98% pure) can be seen in figures S5.III and S5.IV (pH titration) and figures S5.V and S5.VI (NMR spectra). For Na_2AQDS from Combi-Blocks the CO_3^{2-} content is determined to about 20 mole% (Fig. S5.III) from titration, while for Na_2AQDS from TCI, the amount of was determined to be about 9 mole% (Fig. S5.IV). This fits well with the ^1H-NMR spectra in Fig. S5.V, where three characteristic peaks for AQDS were identified. The NMR spectrum for Na_2AQDS from Combi Blocks has many little side peaks which can be attributed to higher percentage of impurities (Fig. S5.V and S5.VI). The colors of these compounds also indicate higher purity for TCI Na_2AQDS. The one from Combi Blocks is dark red, and one from TCI is light purple, and dark red color indicates higher alkalinity of the Na_2AQDS powder purchased from Combi Blocks (Fig. S5.VII). In an additional experiment to confirm the presence of bound CO_3^{2-} in Na_2AQDS, Na_2CO_3 was titrated and is shown as green datapoints in Fig. S5.III. It fully resembles the titration curve for Na_2AQDS.

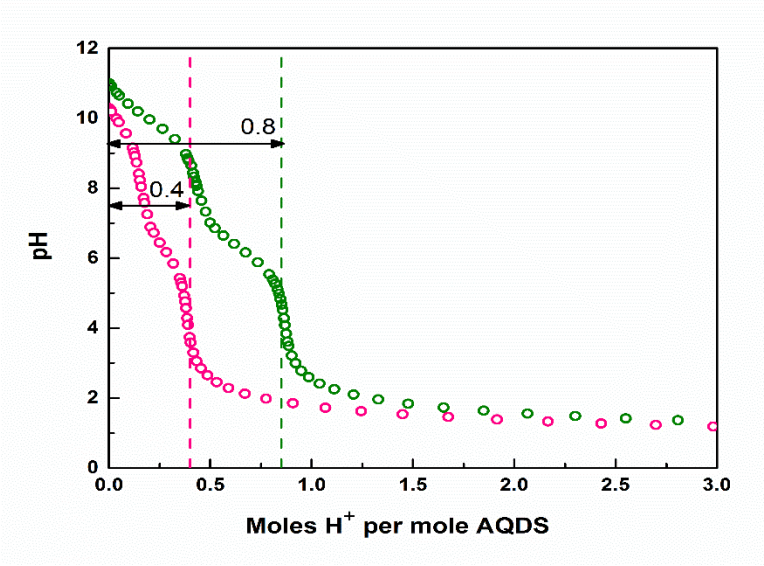

Fig. S5.III Titration curve of oxidised 0.05 M Na_2AQDS (combi-blocks) and 0.01 M Na_2CO_3 (green data points) compaed to titration of 0.05 M Na_2AQDS in water (pink data points) with 0.5 M HCl.

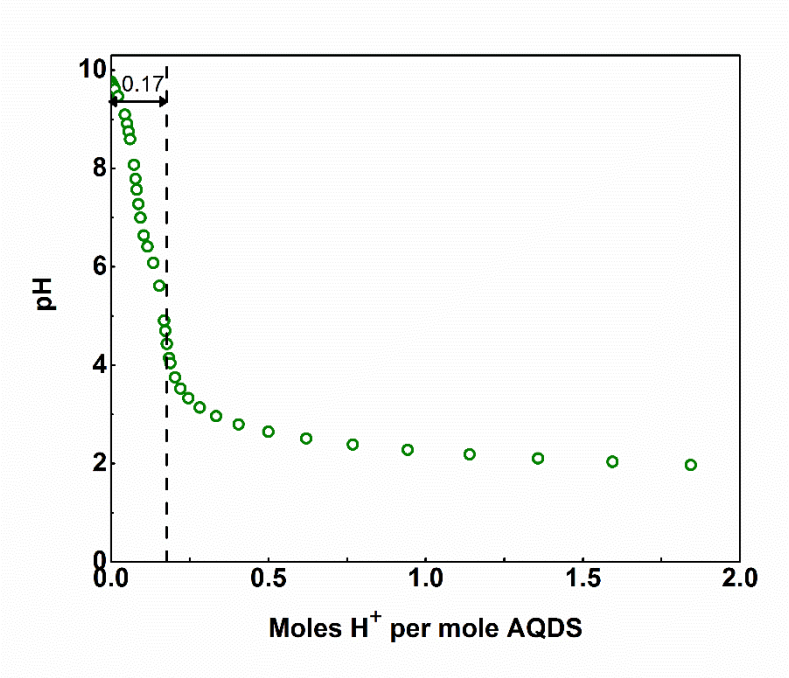

Fig. S5.IV Titration curve of oxidised 0.05 M Na_2AQDS (TCI) with 0.5 M HCl.

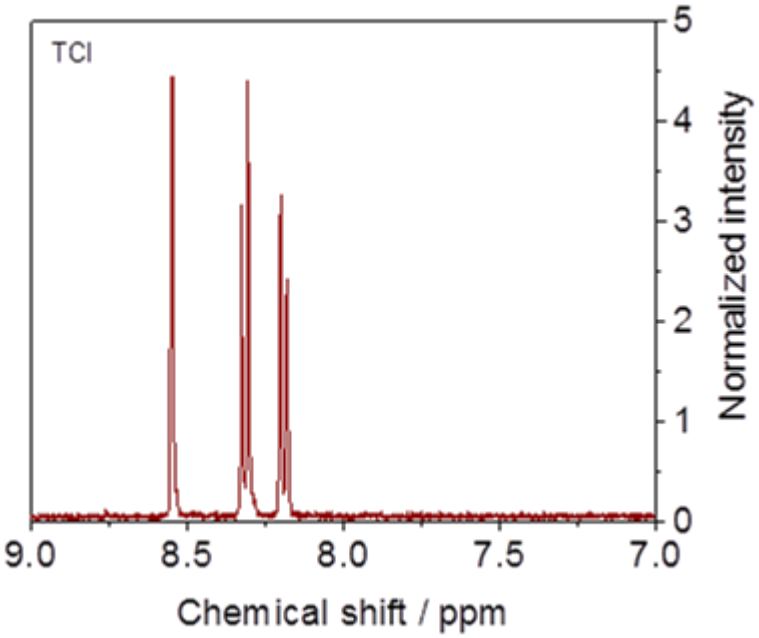

Fig. S5.V ^{1}H-NMR of Na_2AQDS supplied from TCI (97% pure)

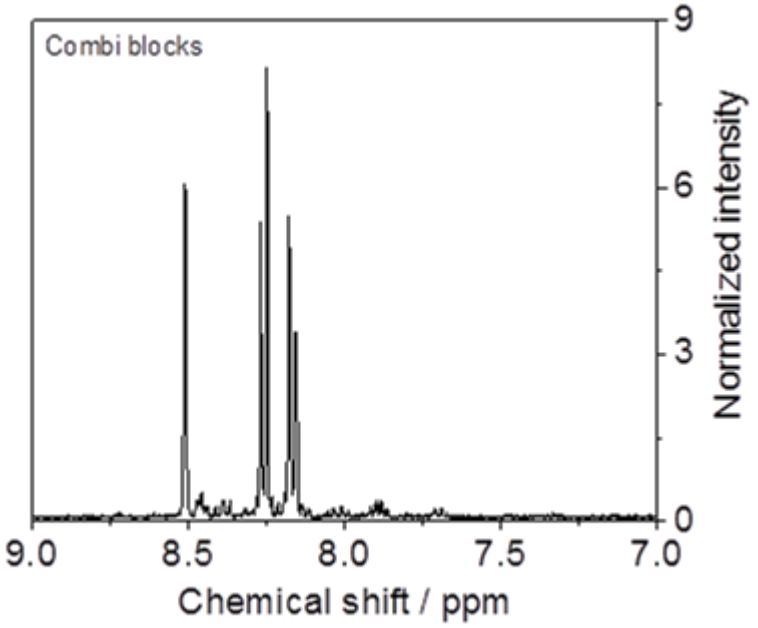

Fig. S5.VI ^{1}H-NMR of Na_2AQDS supplied from combi-blocks (95% pure)

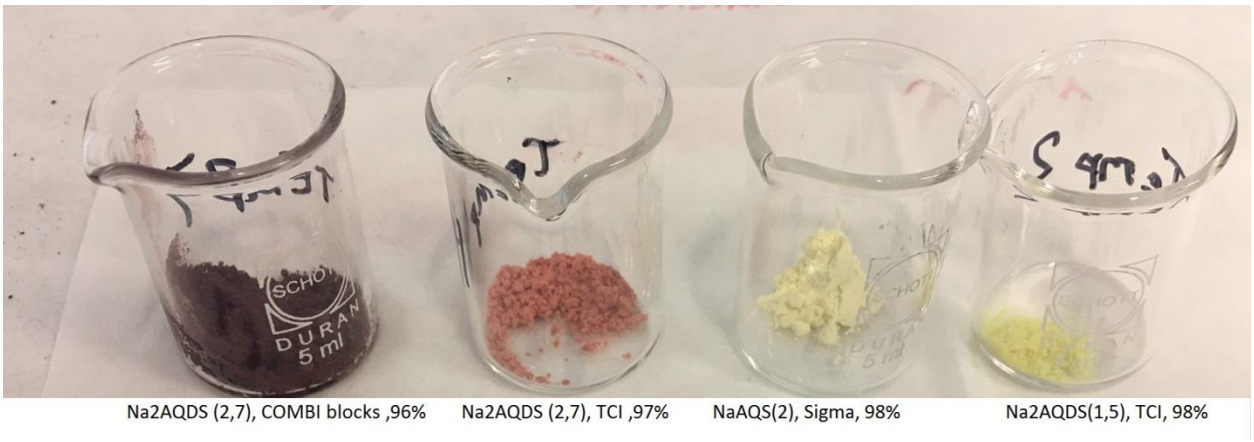

Fig. S5.VII Different quinone compounds with different colors

S6: Experimental capacity as function of current density

16 mA cm^{-2}= 2.197 Ah, 82% of theoretical capacity

24 mA cm^{-2}= 2.09 Ah, 78% of theoretical capacity

32 mA cm^{-2}= 1.983 Ah, 74% of theoretical capacity

40 mA cm^{-2}= 1.876 Ah, 70% of theoretical capacity

48 mA cm^{-2}= 1.394 Ah, 52% of theoretical capacity

S7: Low concentration battery cycling

Low concentration tests (Fig. S7) were conducted using 100 ml of 0.05 M Na_2AQDS in 2 M NH_4Br on the negative side and 100 ml of 0.1 M Br_2 in 2 M NH_4Br aqueous solution on the positive side. Charge/discharge capacity remained at 100% of the theoretical value. As can be seen in the figure below, coulombic efficiency remained over 95% for 50 cycles. The observed capacity loss is 0.02 % per cycle.

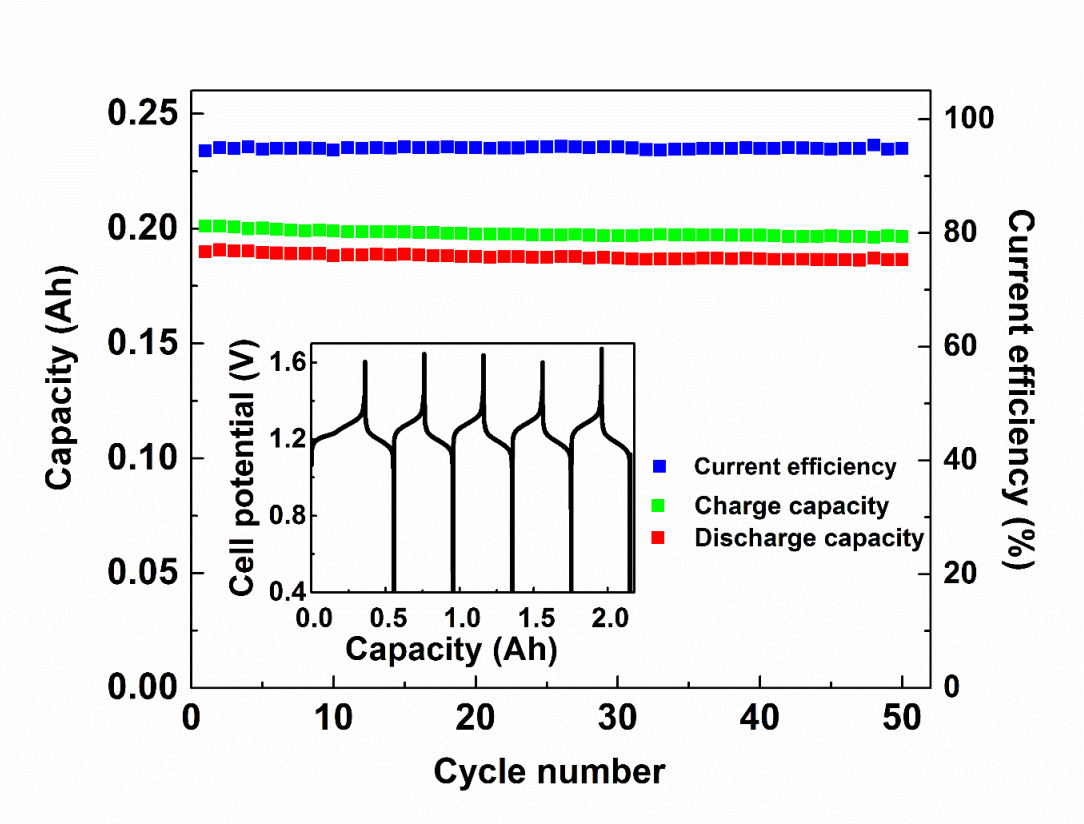

Fig. S7: (a) Charge/discharge capacity and coulombic efficiency versus cycle number with 8 mA cm^{-2}. Inset shows charge/discharge cycles. Experimental conditions: 0.05 M Na_2AQDS in 1.25 M NH_4Br as negative electrolyte and 0.1 M Br_2 in 2 M NH_4Br positive electrolyte using flow rate of 50 mL min^{-1}.

S8: Calculating E_{cell} of the Na_2AQDS/Bromine battery

E_{cell} in Figure 6d in main text is calculated based on the measured potential ($V_{charging,50\%}$) at 50% state of charge during charging and discharging:

$$E_{cell} = V_{charging,50\%} + RI$$

$$E_{cell} = V_{discharging,50\%} - RI$$

The internal resistance contribution is cancelled out by addition of the two equations:

$$E_{cell} = \frac{V_{charging,50\%} + V_{discharging,50\%}}{2}$$

Below is an example of the calculation of E_{cell}:

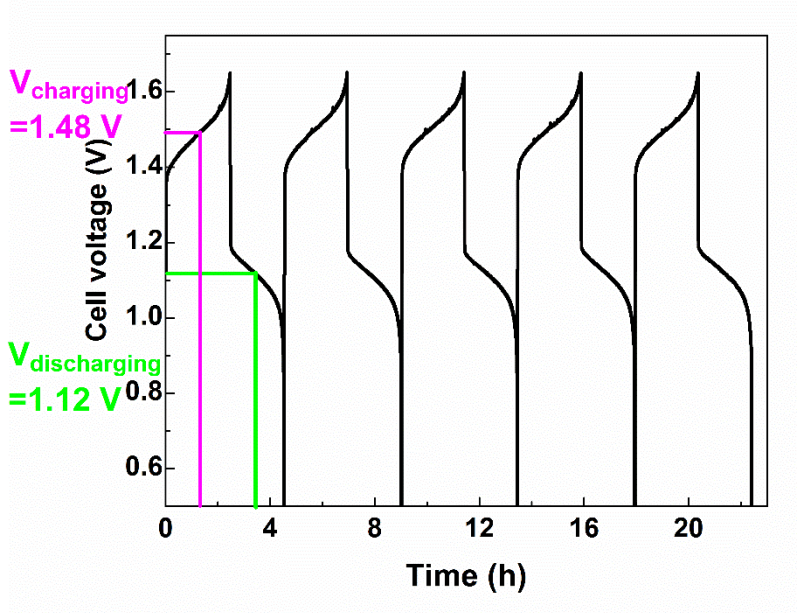

Fig. S8 First five cycles of Na_2AQDS/Br_2 battery. Cell potential's calculation data is shown on first cycle.

S9: pH variation on negative and positive side of batter

Fig. S9.I shows a blank battery test without charging and discharging, but including pumping of the electrolytes. As can be seen, the pH of the negative side is reduced from 8.1 to below 2. One reason for the decrease in pH level, is that bromine crosses over and disproportionate on the negative side and makes it acidic but according to our calculations in section S3, bromine could lower the pH to 2.69 by disproportionation. Therefore, the second reason is high concentration of H^+ on the positive side which makes a high driving force and contributes to further lower the pH of negative side. In order to show the pH variation during charging and discharging, we ran a battery test with the same experimental conditions as Fig. 6 except that the separator Nafion-117 was used instead of Nafion-117-CS. pH of the negative and positive side of the battery was measured every 30 min for the first two cycles which is shown in Fig 7 in the main text. Because of opening/closing of the system for many times during pH measurement, CO_2 escaped to the atmosphere and caused lack of carbonate buffer capacity and significant pH reduction only after 24 hours (Fig. S9.II). As can be seen in Fig. S9.II, pH of the negative side in cycle six at fully discharged state is around four and increases during charging in the next cycle to 8.5 due to consuming

protons. During discharging in cycle seven, reduced Na_2AQDS releases protons to the solution and as there is not enough buffer capacity in the solution, pH is dropped.

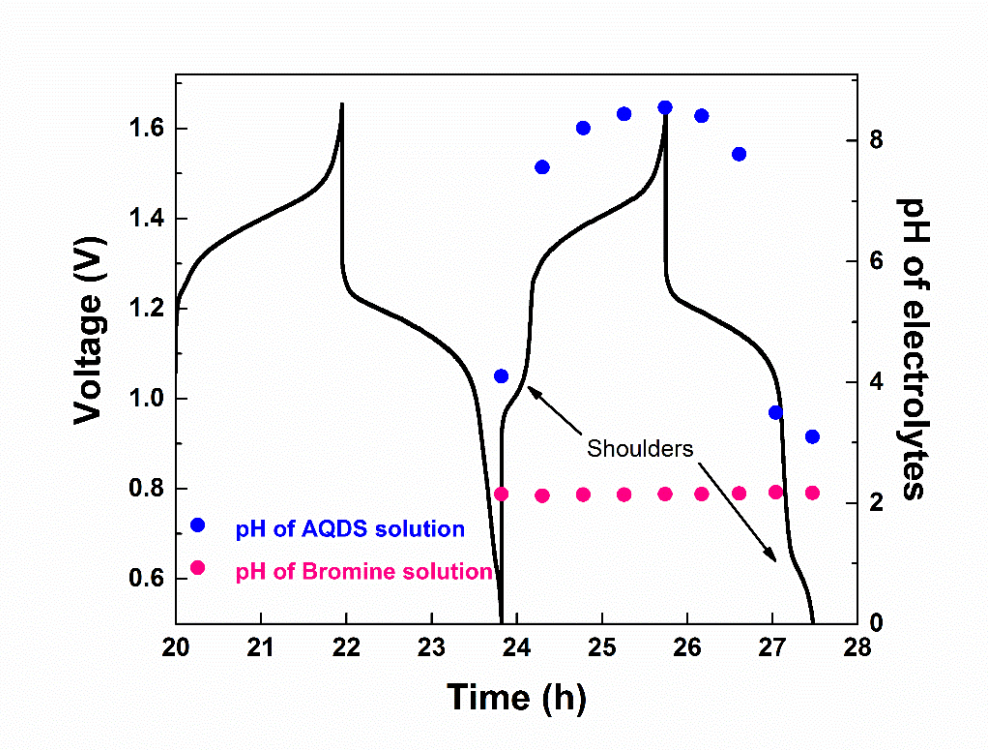

Fig. S9.I pH change during charging and discharging at seventh cycle when carbonate ions were escaped to atmosphere as CO_2 due to opening and closing system every 30 min. Experimental conditions: 0.5 M Na_2AQDS/2 M NH_4Br on the negative side and 0.3 M Br_2/2 M NH_4Br/0.1 M HBr on the positive side. Nafion-117 was used as separator.

The buffer capacity could be restored by bubbling the negative side with CO_2. To do that, we bubbled the solution with CO_2 at fully charged state of cycle eight. Fig. S9.III indicates cycles eight, nine, ten and eleven which in charging/discharging curves show Nernstian behavior once again.

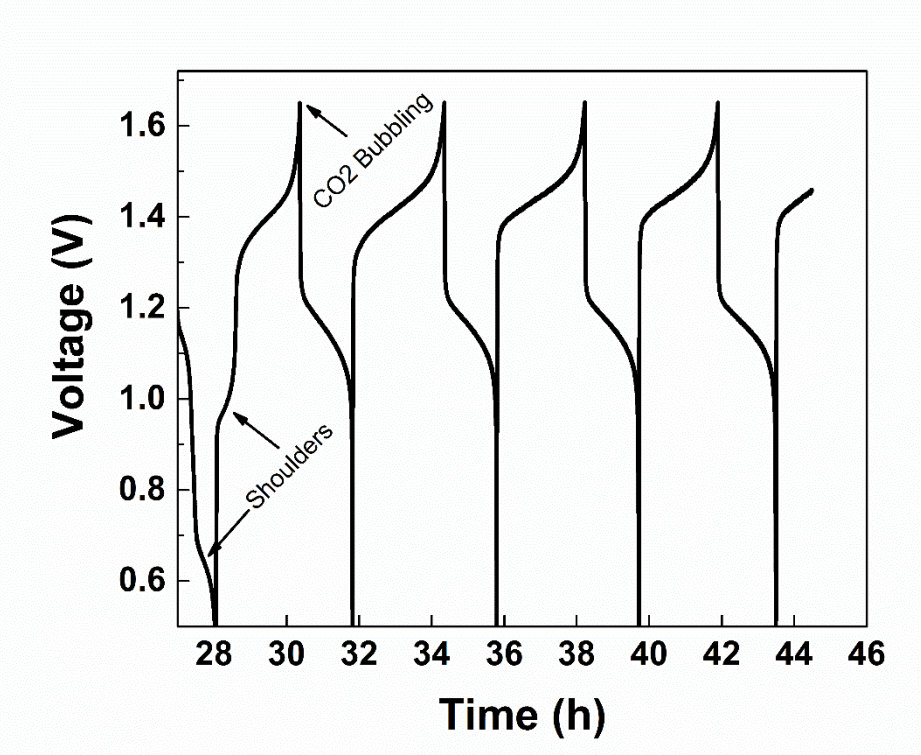

Fig. S9.II charge/discharge cycles after bubbling on the negative side with CO_2. Charging is started at eighth cycle in the rest of Fig. S9.II. Experimental conditions: 0.5 M Na_2AQDS/2 M NH_4Br on the negative side and 0.3 M Br_2/2 M NH_4Br/0.1 M HBr on the positive side. Nafion-117 was used as separator.

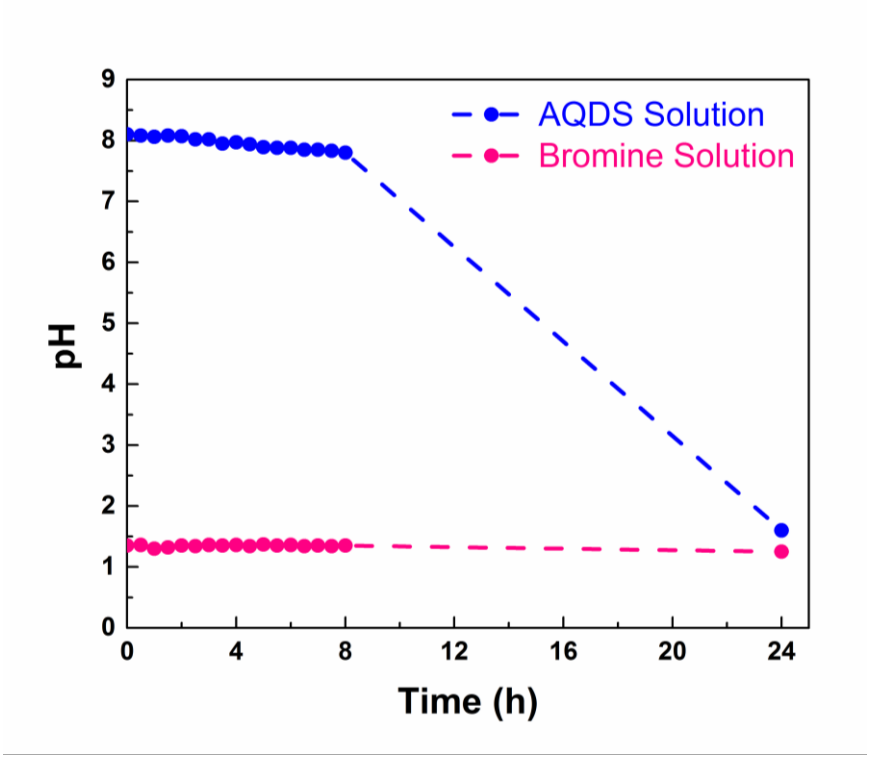

Fig. S9.III pH versus time for a blank test without charging and discharging. pH was measured for 8 hours in every 30 min and then after 24 hours. Experimental conditions: 0.5 M Na_2AQDS/2 M NH_4Br on the negative side and 0.3 M Br2/2 M NH_4Br/0.1 M HBr on the positive side. Nafion-117 was used as separator.

References

1. N. N. E. Greenwood, A, Chemistry of the elements, Butterworth-Heineman, 2nd Edition edn., 1997.
2. R. Weast, CRC handbook of Chemistry and Physics, The Chemical Rubber Co, Fifty-Second Edition edn., 1971-1972.
3. H. Freiser and Q. Fernando, Ionic equilibria in analytical chemistry, John Wiley & Sons Inc., New York, 1963.
4. G. Jones and S. Baeckström, Journal of the American Chemical Society, 1934, **56**, 1517-1523.
5. T. Michalowski, Journal of chemical education, 1994, **71**, 560.
6. G. R. Compton, Banks, E.C., Understanding Voltammetry, Imperial College Press, 2nd Edition edn., 2010.